First-principles investigation of structural stability, mechanical properties and electronic structure of Ru1−xRexB2 and Re1−xRuxB2 borides

ARTICLE *in* COMPUTATIONAL MATERIALS SCIENCE · MARCH 2014

Impact Factor: 2.13 · DOI: 10.1016/j.commatsci.2014.03.029

3 AUTHORS, INCLUDING:

Yong Pan
Southwest Petroleum University
32 PUBLICATIONS **72** CITATIONS

Computational Materials Science 89 (2014) 19–23

Contents lists available at ScienceDirect

Computational Materials Science

journal homepage: www.elsevier.com/locate/commatsci

First-principles investigation of structural stability, mechanical properties and electronic structure of $Ru_{1-x}Re_xB_2$ and $Re_{1-x}Ru_xB_2$ borides

Y. Pan [a,*], H.W. Huang [b], W.M. Guan [a]

[a] State Key Laboratory of Advanced Technologies for Comprehensive Utilization of Platinum Metals, Kunming 650106, PR China
[b] Department of Mechanical Engineering, Luzhou Vocational and Technical College, Luzhou 646005, PR China

ARTICLE INFO

Article history:
Received 15 December 2013
Received in revised form 21 February 2014
Accepted 16 March 2014

Keywords:
Ab initio calculations
Phase stable
Elastic properties
B/*G* ratio

ABSTRACT

The structural stable, elastic modulus and *B*/*G* ratio of $Ru_{1-x}Re_xB_2$ and $Re_{1-x}Ru_xB_2$ borides are studied by using first-principles approach. The calculated formation enthalpies show that the $Re_{1-x}Ru_xB_2$ is more stable than that of $Ru_{1-x}Re_xB_2$. The bulk and shear modulus of $Ru_{1-x}Re_xB_2$ and $Re_{1-x}Ru_xB_2$ borides increase with increasing Re concentration. The *B*/*G* ratio of $Ru_{1-x}Re_xB_2$ increases along the Re concentration decreases. However, there is a convex hull ($x = 0.25$) in $Re_{1-x}Ru_xB_2$. The calculated *B*/*G* ratio of $Re_{0.75}Ru_{0.25}B_2$ (1.23) is lower than that of ReB_2 (1.29), indicating that the $Re_{1-x}Ru_xB_2$ has potential binary alloy superhard materials in this region ($0 < x < 0.375$). This discrepancy is originated from the hybridization between Re and B atoms is stronger than between Ru and B atoms.

1. Introduction

Since the ReB_2 was successfully synthesized by arc-melting method and the average hardness is about of 48 GPa with a load of 0.48 N [1], the transition metal borides (TMBs) as the potential superhard materials candidates have great interest due to the high bulk modulus, high shear modulus, high hardness, ultra-incompressible and a degree of metallic behavior et al. [2–7]. However, numerous TMBs are not superhard materials. Therefore, to search for new superhard materials is necessary.

Over the past years, the extensive theoretical and experimental mainly focused on the structural and mechanical properties of diborides (TMB_2). According to the new design principle, the potential superhard materials should be meet two conditions: high valence electronic density and bond covalency [8]. The boron-rich TMBs is easily to form superhard material. Unfortunately, the boron-rich TMBs is very difficult to synthesize by experimental method.

Recently, Krauss et al. [9] have been investigated the relationship between hardness and ultra-incompressible of TMBs. They found that the hardness of $Os_{0.5}W_{0.5}B_2$ is about of 40.4 GPa, which is bigger than that WB_2 and OsB_2. On the other hand, the crystal structural, elastic modulus, hardness and electronic structure of $Os_{0.5}W_{0.5}B_2$, $Re_{0.5}W_{0.5}B_2$ and $Os_{0.5}Re_{0.5}B_2$ are studied by first-principle approach [10]. The calculated results shown that the intrinsic hardness of these binary alloy borides are bigger than 40 GPa. Obviously, these studies open up a novel route for the search of new superhard materials. However, studies on the structural and mechanical properties of binary alloy borides with unusual composition are very scarce.

In order to explore the binary alloy high hard borides, in this paper, the structural stability, elastic modulus and electronic structure of $Ru_{1-x}Re_xB_2$ and $Re_{1-x}Ru_xB_2$ systems are investigated by first-principles approach. The main purpose of this work is to propose some helpful for the future search of the new superhard materials.

2. Computational details

For $Ru_{1-x}Re_xB_2$ and $Re_{1-x}Ru_xB_2$ systems, the structure of RuB_2 and ReB_2 should be firstly considered. As we know, the RuB_2 in an orthorhombic structure (Space group: Pmmm, No: 59) with lattice parameters: $a = 4.645$ Å, $b = 2.865$ Å and $c = 4.045$ Å [11,12]. The Ru and B atoms occupy the 2a (0.0114, 0.2500, 0.8773) and 4f (0.1489, 0.0776, 0.3940) sites, respectively. The ReB_2 is a hexagonal structure with lattice parameters: $a = b = 2.900$ Å and $c = 7.478$ Å (Space group: P63/mmc, No: 194) [1]. The Re and B atoms occupy the 2c (0.3333, 0.6667, 0.2500) and 4f (0.3333, 0.6667, 0.5483) sites, respectively.

For $Ru_{1-x}Re_xB_2$ ($0 \leqslant x \leqslant 1$), nine different types of Re concentrations including 0, 0.125, 0.250, 0.375, 0.500, 0.625, 0.750, 0.875 and

* Corresponding author. Tel.: +86 871 68328950; fax: +86 871 68328945.
E-mail address: y_pan@ipm.com.cn (Y. Pan).

http://dx.doi.org/10.1016/j.commatsci.2014.03.029
0927-0256/

1 are considered, respectively. The Ru atom is randomly substituted by Re atoms while the RuB_2 as the host structure. To obtain stable structure, all symmetrical distinct $Re_{1-x}Ru_xB_2$ configurations are calculated by first-principles based on the total energy minimization scheme, the same way as the $Ru_{1-x}Re_xB_2$ system.

The first-principles total energy calculations were performed with density functional theory as implemented using the *ab initio* simulation Package (VASP) [13,14]. The exchange correlation functional was taken into account through the generalized gradient approximation (GGA) [15] with the Burke Ernzerhof functionals (PBE) exchange correlation functional [16]. The interaction between ions and electrons was described using the Vanderbilt ultra-soft pseudopotential. A plane-wave basis set for electron wave function with cut-off energy of 400 eV was used. Integrations in the brillouin zone were performed using special *k*-point generated with $7 \times 11 \times 16$ for these structures [17] . During the structural optimization, no symmetry and no restriction were constrained for the unit-cell shape, volume and atomic position. The structural relaxation was stopped until the total energy, the max force and the max displacement were less than 1×10^{-5} eV/atom, 0.001 eV/Å, and 0.001 Å, respectively.

3. Results and discussion

3.1. Structural stability

For binary alloy borides, many properties such as structural stability, elastic properties and hardness mainly depend on the configuration. The system with N atoms has 2^N possible number of configurations. Obviously, it is an astronomically number when N is large. According to the symmetrical operation, the number of $Ru_{1-x}Re_xB_2$ and $Re_{1-x}Ru_xB_2$ systems including 8 TM atoms and 16 boron atoms is reduced to 34 distinct configurations, respectively. The formation enthalpies can be calculated as follows:

For $Re_{1-x}Ru_xB_2$ borides

$$\Delta H(x) = E(Re_{1-x}Ru_xB_2) - (1-x)E(ReB_2) - xE(RuB_2) \quad (1)$$

For $Ru_{1-x}Re_xB_2$ borides

$$\Delta H(x) = E(Ru_{1-x}Re_xB_2) - (1-x)E(RuB_2) - xE(ReB_2) \quad (2)$$

where $E(Re_{1-x}Ru_xB_2)$, $E(Ru_{1-x}Re_xB_2)$, $E(ReB_2)$ and $E(RuB_2)$ are the calculated total energies of the $Re_{1-x}Ru_xB_2$, $Ru_{1-x}Re_xB_2$, pure ReB_2 and RuB_2, respectively.

The calculated lattice parameter and volume of RuB_2, $Re_{0.5}Ru_{0.5}B_2$ and ReB_2 are listed in Table 1. It can be seen that the calculated lattice parameter and volume of RuB_2 and ReB_2 are in good agreement with the previous experimental data and theoretical results.

Table 1
The calculated lattice parameters (in Å) and volume (in $Å^3$) of RuB_2, $Re_{0.5}Ru_{0.5}B_2$ and ReB_2, respectively.

Phase	Method	Space group	*a*	*b*	*c*	*V*
RuB_2	Cal	Pmmm	4.747	2.870	4.047	53.992
	Exp[a]		4.645	2.865	4.045	
	Theo[b]		4.649	2.890	4.039	
$Re_{0.5}Ru_{0.5}B$	Cal		2.916		7.397	54.480
ReB_2	Cal	P63/mmc	2.912		7.502	54.976
	Exp[c]		2.900		7.478	
	Theo[d]		2.875		7.421	
	Theo[e]		2.870		7.398	

[a] Ref. [11].
[b] Ref. [18].
[c] Ref. [19].
[d] Ref. [20].
[e] Ref. [21].

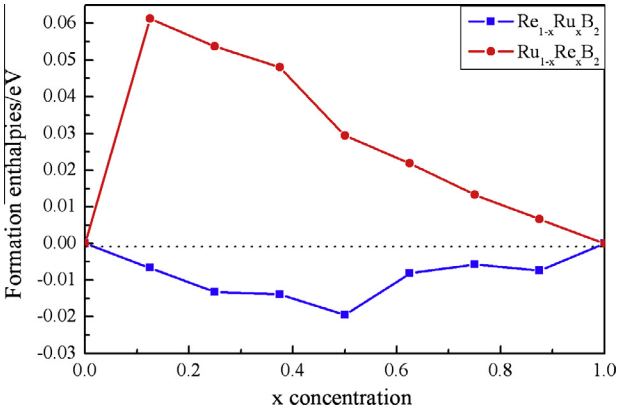

Fig. 1. Calculated formation enthalpies of $Re_{1-x}Ru_xB_2$ and $Ru_{1-x}Re_xB_2$ borides in a unit cell of 24 atoms.

In addition, the calculated *a*- axis of $Re_{0.5}Ru_{0.5}B_2$ is bigger than that the corresponding axis of ReB_2 in contrast to the *c*- axis for former is lower than the latter, indicating that the hybridization between B and TM atoms along *c*- axis is stronger than that of *a*- axis.

The calculated formation enthalpies of $Ru_{1-x}Re_xB_2$ and $Re_{1-x}Ru_xB_2$ borides are shown in Fig. 1. The red[1] and blue lines represent the formation enthalpies of $Ru_{1-x}Re_xB_2$ and $Re_{1-x}Ru_xB_2$ borides, respectively. As shown in Fig. 1, the positive mixing enthalpies of $Ru_{1-x}Re_xB_2$ indicate the metastable structure at ground state, while the large positive mixing enthalpy is about of 0.061 eV/atom. Obviously, the energetic driving force results in phase separation in this binary alloy borides. Therefore, we suggest that Ru atom is difficult replaced by Re atom when RuB_2 as the host structure.

It is worth to notice that the calculated formation enthalpies of $Re_{1-x}Ru_xB_2$ are negative, implying that the random $Re_{1-x}Ru_xB_2$ configurations are stable structures at ground state. On the other hand, the values of formation enthalpy of $Re_{1-x}Ru_xB_2$ are lower than that of $Ru_{1-x}Re_xB_2$. These results indicate that 5*d*- Re atoms is easily replaced by 4*d*- Ru atoms when ReB_2 as the host structure. Unfortunately, there are no experimental or other theoretical results for comparison. We hope that our calculated results can be provided helpful to the future experimental.

Moreover, the calculated results show that the hybridization of $Re_{1-x}Ru_xB_2$ focus on the Re–B and B–B atoms in ReB_2- rich region when $x < 0.5$. Although the doped Ru atom changes the localize hybridization between B and TM atoms, the structural type of the $Re_{1-x}Ru_xB_2$ borides reserve the ReB_2 host structure. This is no surprising that the Re atom play a key role in this region. When $x > 0.5$, the $Re_{1-x}Ru_xB_2$ undergoes a phase transition from hexagonal to orthorhombic structure. As shown in Fig. 1, the phase transition is at $x = 0.5$ (convex hull), and the lowest negative enthalpy is about of −0.020 eV/atom, meaning that the $Re_{0.5}Ru_{0.5}B_2$ is the most stable structure. We suggest that this phase transition is responsible for the interaction between Ru and B atoms with increasing the Ru concentration. Then, the Ru–B bonds play an important role in $Re_{1-x}Ru_xB_2$ borides.

Following, the structural characteristic of $Re_{0.5}Ru_{0.5}B_2$ should be discussed. The $Re_{0.5}Ru_{0.5}B_2$ structure with alternative stacked Re and Ru layers along (001) plane is shown in Fig. 2. We found that the $Re_{0.5}Ru_{0.5}B_2$ reserves the hexagonal ReB_2 structure. In going from ReB_2 to $Re_{0.5}Ru_{0.5}B_2$, the decrease in *c*- axis is ≈ 1.08 % whereas the increase in *a*- axis is ≈ 0.55 %. The decrease in *c*- axis reflects the strong hybridization between B and Ru atoms and then forms Ru–B covalent bonds. Furthermore, the $Re_{0.5}Ru_{0.5}B_2$ structure is consist

[1] For interpretation of color in Fig. 1, the reader is referred to the web version of this article.

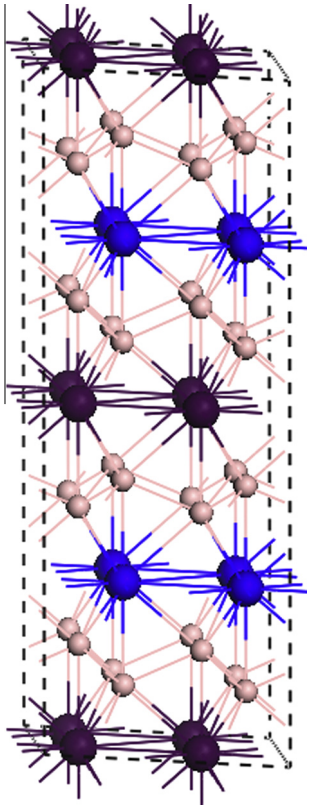

Fig. 2. The structure of $Re_{0.5}Ru_{0.5}B_2$. Re, Ru and B atoms are in purple, blue and orange, respectively. (For interpretation of the references to color in this figure legend, the reader is referred to the web version of this article.)

with three types of bonds: Re–B, Ru–B and B–B covalent bonds. The calculated bond lengths of Re–B (2.217 Å), Ru–B (2.212 Å) and B–B (1.835 Å) bonds, which are in good agreement with the previous theoretical results [22–24]. Obviously, the arrangement of Ru–B and Re–B covalent bonds in $Re_{0.5}Ru_{0.5}B_2$ can compensate the bond strength of Ru–B bonds (see Fig. 2). In particularly, the 3D network covalent bonds including Re–B, Ru–B and B–B covalent bonds improve its stability.

In order to reveal the nature of structural stability of $Re_{0.5}Ru_{0.5}B_2$ compared to the ReB_2 and RuB_2, the electronic structure of $Re_{0.5}Ru_{0.5}B_2$, ReB_2 and RuB_2 is discussed. According to the band filling theory [25], the material stability is related to the number

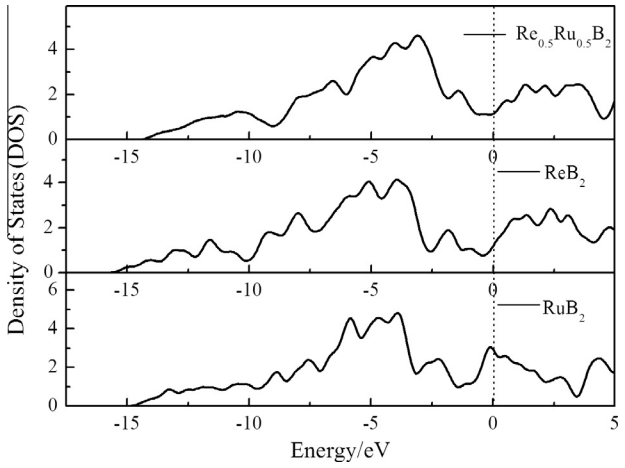

Fig. 3. The total density of states (DOS) of RuB_2, ReB_2 and $Re_{0.5}Ru_{0.5}B_2$, respectively.

of filling bonding or antibonding states. The band filling theory including two factors: W_{occ}, the width of occupied states, and W_b, the width of bonding states. Therefore, the W_{occ}/W_b ratio can evaluate the material stability. The general trend is, the bigger the W_{occ}/W_b ratio, the more stable the materials.

The calculated density of states (DOS) including W_{occ}, W_b, and W_{occ}/W_b ratio are given in Fig. 3 and Table 2, respectively. As seen in Fig. 3 and Table 2, the W_{occ} of $Re_{0.5}Ru_{0.5}B_2$ is bigger than that of RuB_2, and is smaller than ReB_2. However, the W_b of $Re_{0.5}Ru_{0.5}B_2$ is smaller than that of RuB_2 and ReB_2. Obviously, the W_{occ}/W_b ratio of $Re_{0.5}Ru_{0.5}B_2$ is bigger than the RuB_2 and ReB_2, indicating that the $Re_{0.5}Ru_{0.5}B_2$ is more stable than that of ReB_2 and RuB_2. This result is consistent with the calculated formation enthalpies.

3.2. Mechanical properties

Elastic modulus such as bulk modulus and shear modulus are important mechanical parameter because they check the mechanical stability, strength, hardness and brittle or ductile behavior. In order to search for high hard binary alloy borides, therefore, the elastic modulus should be analyzed and discussed.

Fig. 4 presents the calculated bulk and shear modulus of $Ru_{1-x}Re_xB_2$ and $Re_{1-x}Ru_xB_2$, respectively. We firstly observe that the calculated bulk and shear modulus of RuB_2 and ReB_2 are in excellent agreement with the previous theoretical results [26,27]. Furthermore, the bulk and shear modulus of $Ru_{1-x}Re_xB_2$ increase as the Re concentration increases. In contrast, the bulk and shear modulus of $Re_{1-x}Ru_xB_2$ decrease with increasing of Ru concentration. This discrepancy is due to the fact that the hybridization between B and Re atoms is stronger than between B and Ru atoms. Therefore, we conclude that the elastic modulus of these binary alloy borides mainly depend on the 5*d*- Re concentration.

The calculated elastic constants of RuB_2, $Re_{0.5}Ru_{0.5}B_2$ and ReB_2 are listed in Table 3, together with the previous theoretical results. It can be seen that the calculated elastic constants of these borides satisfy the Born stability criteria, meaning that the mechanical stability at ground state. In addition, the calculated elastic constants of RuB_2 and ReB_2 are in excellent agreement with other theoretical data. Moreover, we found that the calculated elastic constants C_{11} and C_{33} of $Re_{0.5}Ru_{0.5}B_2$ are bigger than that of RuB_2, and are smaller than that of ReB_2, indicating that the resistance to deformation along *a*- axis and *c*- axis for $Re_{0.5}Ru_{0.5}B_2$ is stronger than that of RuB_2, and is more weak than that of ReB_2. The main reason is that the hybridization between B and Re atoms is stronger than between B and Ru atoms.

The calculated bulk modulus, shear modulus, Young's Modulus, Poisson ratio, δ and B/G ratio of RuB_2, $Re_{0.5}Ru_{0.5}B_2$ and ReB_2 are listed in Table 4. The bulk and shear modulus in this paper are calculated by Voigt-Reuss-Hill approximation [28]. It is obvious that the calculated bulk modulus, shear modulus and Young's Modulus of $Re_{0.5}Ru_{0.5}B_2$ are bigger than the corresponding elastic modulus of RuB_2 and are lower than the corresponding elastic modulus of ReB_2. These results indicate that the 5*d*- Re atom can enhance the resistance to the shape and shear deformation.

According to the Pugh rule [29], the brittle or ductile behavior of a material is determined by the ratio of bulk and shear modulus.

Table 2
The width of occupied states W_{occ}, the bonding states W_b and W_{occ}/W_b of RuB_2, ReB_2 and $Re_{0.5}Ru_{0.5}B_2$, respectively.

Phase	W_{occ}	W_b	W_{occ}/W_b
RuB_2	14.86	14.40	1.04
ReB_2	16.07	15.54	1.03
$Re_{0.5}Ru_{0.5}B_2$	15.42	14.27	1.08

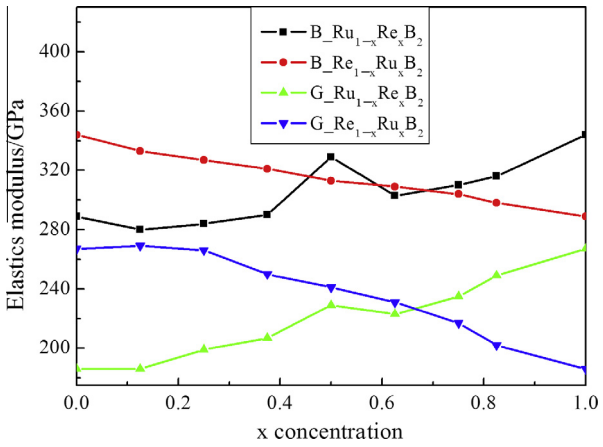

Fig. 4. The calculated bulk and shear modulus of $Re_{1-x}Ru_xB_2$ and $Ru_{1-x}Re_xB_2$, respectively.

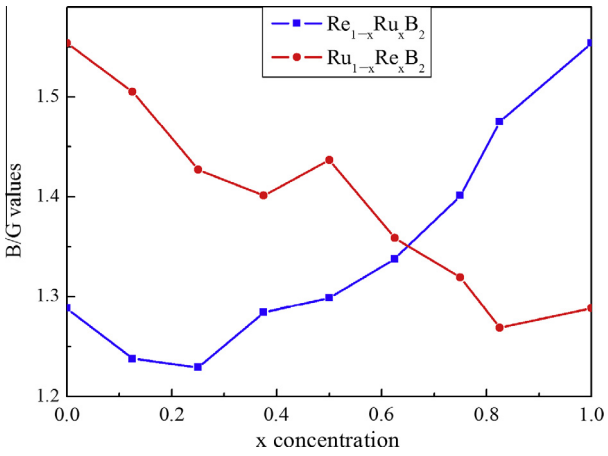

Fig. 5. The calculated B/G ratio of $Re_{1-x}Ru_xB_2$ and $Ru_{1-x}Re_xB_2$, respectively.

Table 3
The calculated elastic constants, C^{ij} (in GPa) of RuB_2, $Re_{0.5}Ru_{0.5}B_2$ and ReB_2, respectively.

Phase	Method	C_{11}	C_{12}	C_{13}	C_{22}	C_{23}	C_{33}	C_{44}	C_{55}	C_{66}
RuB_2	Cal	519	188	146	458	125	706	118	230	176
	Theo[a]	495	162	131	413	110	657	127	223	172
$Re_{0.5}Ru_{0.5}B_2$		559	147	125			902	227		206
ReB_2	Cal	613	178	125			1015	256		217
	Theo[b]	682	188	131			1118	290		266

[a] Ref. [18].
[b] Ref. [21].

The critical value which separates ductile and brittle materials is around 1.75. If $B/G > 1.75$, a material behavior exhibits a ductile manner, and versa, if $B/G < 1.75$, a material demonstrates brittleness. It is well known that the bulk and shear modulus represent the resistance to shape and plastic deformation under applied load. Therefore, the B/G ratio indirectly reflects the trend of hardness. The general trend is, the lower the B/G ratio, the higher the brittleness and hardness.

The calculated B/G ratio of $Ru_{1-x}Re_xB_2$ and $Re_{1-x}Ru_xB_2$ are shown in Fig. 5. It can be seen that the B/G ratio of ReB_2 (1.29) is lower than that of RuB_2 (1.55), indicating that the brittle behavior of ReB_2 is stronger than that of RuB_2, which is consistent with the analysis of measured hardness. We note that the calculated B/G ratio of these binary alloy borides is lower than 1.75. Therefore, these binary alloy borides exhibit brittle behavior and have potential high hardness. Furthermore, the calculated B/G ratios of $Ru_{1-x}Re_xB_2$ rapidly decrease with increasing the Re concentration, except for $x = 0.5$. That is to say, the intrinsic hardness at Re- rich region is higher than that of Ru- rich region. However, we observe that there is a convex hull at $x = 0.25$ in $Re_{1-x}Ru_xB_2$, and the calculated B/G ratio in region of $0 < x < 0.375$ is lower than that of ReB_2. It is worth to mention that the calculated B/G ratio of $Re_{0.75}Ru_{0.25}B_2$ (1.23) is lower than that of ReB_2 (1.29), implying that this $Re_{0.75}Ru_{0.25}B_2$ has potential high hardness.

Table 4
The calculated bulk Modulus, B (in GPa), shear modulus, G (in GPa), Young's Modulus, E (in GPa), Poisson ratio, δ and B/G ratio of RuB_2, $Re_{0.5}Ru_{0.5}B_2$ and ReB_2, respectively.

Phase	Method	B	G	E	δ	B/G
RuB_2	Cal	286	179	444	0.241	1.598
	Theo[a]	263	182	418		
$Re_{0.5}Ru_{0.5}B_2$	Cal	307	236	564	0.194	1.301
ReB_2	Cal	338	261	623	0.193	1.295
	Theo[b]	370	295	698		1.254

[a] Ref. [18].
[b] Ref. [21].

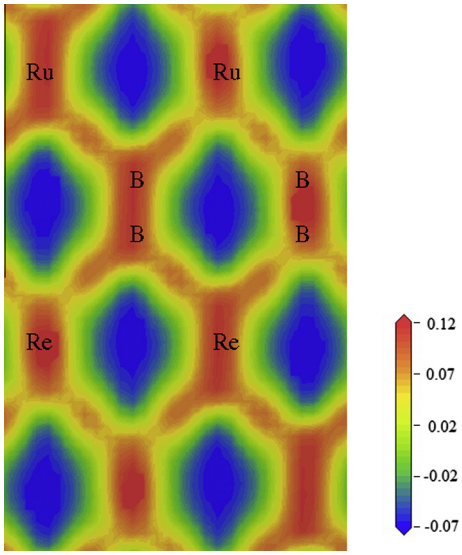

Fig. 6. The different charge density contour plots of $Re_{0.5}Ru_{0.5}B_2$ along the (010) plane.

3.3. Charge density

To reveal the nature of bond characteristic of $Re_{0.5}Ru_{0.5}B_2$, the charge density of $Re_{0.5}Ru_{0.5}B_2$ along the (010) plane is shown in Fig. 6, where the critical feature are labeled. From Fig. 6, the hybridization between B and Ru, Re and B atoms, implying that the directional Ru–B, Re–B and B–B covalent bonds are formed in this binary ally borides. It is worth to notice that the value of electronic localization function (ELF) between Re and B atoms is bigger than between Ru and B atoms, indicating that the hybridization about Re–B covalent bond is stronger than that of Ru–B covalent bond. There is a reason why the Re atom can improve its resistance shape and plastic deformation.

4. Conclusions

In summary, we presented first-principle density functional theory to investigate the structural stability, elastic modulus and B/G

ratio of $Ru_{1-x}Re_xB_2$ and $Re_{1-x}Ru_xB_2$ borides. The calculated formation enthalpies show that the $Re_{1-x}Ru_xB_2$ is more stable than that of $Ru_{1-x}Re_xB_2$, and the $Re_{0.5}Ru_{0.5}B_2$ is the most stable structure because it has lowest formation enthalpy about of −0.020 eV/atom. According to the band filling theory, the W_{occ}/W_b ratio of $Re_{0.5}Ru_{0.5}B_2$ is bigger than that of ReB_2 and RuB_2, which is consistent with the calculated formation enthalpies. The bulk and shear modulus are related to the Re concentration. In addition, the calculated B/G ratio of $Ru_{1-x}Re_xB_2$ and $Re_{1-x}Ru_xB_2$ are lower than 1.75. There is a convex hull ($x = 0.25$) in $Re_{1-x}Ru_xB_2$ borides and the $Re_{0.75}Ru_{0.25}B_2$ has lowest B/G ratio about of 1.23. The present results give hints for designing the binary alloy boride superhard materials and should be used to stimulate further experimental and theoretical work.

Acknowledgements

Financial support by the National Natural Science Foundation of China (Grant Nos. 50525204, 50832001 and 50902057) and the Important Natural Science Foundation of Yunnan (Grant No. 2009CD 134) are gratefully acknowledged.

References

[1] H.Y. Chung, M.B. Weinberger, J.B. Levine, A. Kavner, J.M. Yang, S.H. Tolbert, R.B. Kaner, Science 316 (2007) 436.
[2] J. Yang, H. Sun, C.F. Chen, J. Am. Chem. Soc. 130 (2008) 7200.
[3] B.J. Suh, X. Zong, Y. Singh, A. Niazi, D.C. Johnston, Phys. Rev. B 76 (2007) 144511.
[4] J.A. Rau, A. Latini, Chem. Mater. 21 (2009) 1407.
[5] A. Latini, J.V. Rau, R. Teghil, A. Generosi, V.R. Alberini, Appl. Mater. Inter. 2 (2010) 581.
[6] M.M. Zhong, X.Y. Kuang, Z.H. Wang, P. Shao, L.P. Ding, X.F. Huang, J. Phys. Chem. C 117 (2013) 10643.
[7] Y. Pan, W.T. Zheng, W.M. Guan, K.H. Zhang, X.F. Fan, J. Solid State Chem. 207 (2013) 29.
[8] R.B. Kaner, J.J. Gilman, S.H. Tolbert, Science 308 (2005) 1268.
[9] Q.F. Gu, G. Krauss, W. Steurer, Adv. Mater. 20 (2008) 3620.
[10] X.P. Du, Y.X. Wang, Phys. Status Solidi-Rapid Res. Lett. 3 (2009) 106.
[11] B. Aronsson, Acta Chem. Scand. 17 (1963) 2036.
[12] M. Frotscher, M. Hölzel, B. Albert, Z. Angew, Math. Mech. 636 (2010) 1783.
[13] G. Kresse, J. Furthmüller, Phys. Rev. B 54 (1996) 11169.
[14] G. Kresse, D. Joubert, Phys. Rev. B 59 (1999) 1758.
[15] J.P. Perdew, J.A. Chevary, S.H. Vosko, K.A. Jackson, M.R. Pederson, D.J. Singh, C. Fiolhais, Phys. Rev. B 46 (1992) 6671.
[16] J.P. Perdew, K. Burke, M. Ernzerhof, Phys. Rev. Lett. 77 (1996) 3865.
[17] H.J. Monkhorst, J.D. Pack, Phys. Rev. B 13 (1976) 5188.
[18] P. Yong, Z. Kunhua, G. Weiming, C. Song, Rare Metal Mat. Eng. 41 (2012) 2086.
[19] S. Aydin, M. Simsek, Phys. Rev. B 80 (2009) 134107.
[20] E. Deligoz, K. Colakoglu, Y.O. Ciftci, Chin. Phys. B 21 (2012) 106301.
[21] Y. Pan, W.T. Zheng, W.M. Guan, K.H. Zhang, S.S. Yu, X.Y. Hu, Comput. Mater. Sci. 82 (2014) 12.
[22] Y.X. Wang, Appl. Phys. Lett. 91 (2007) 101904.
[23] B.P.T. Fokwa, J.V. Appen, R. Dronskowski, Chem. Commun. (2006) 4419.
[24] M.B. Weinberger, J.B. Levine, H.Y. Chung, R.W. Cumberland, H.I. Rasool, J.M. Yang, R.B. Kaner, Chem. Mater. 21 (2009) 1915.
[25] J.h. Xu, A.J. Freeman, Phys. Rev. B 40 (1989) 11927.
[26] X.F. Hao, Y.H. XU, Z.J. Wu, D.F. ZHou, X.J. Liu, J. Meng, J. Alloys. Compd. 453 (2008) 413.
[27] M.R. Koehler, V. Keppens, B.C. Sales, R.Y. Jin, D. Mandrus, J. Phys. D Appl. Phys. 42 (2009) 095414.
[28] R. Hill, Proc. Phys. Soc. A 65 (1952) 349.
[29] S.F. Pugh, Philos. Mag. A 45 (1954) 823.